JOURNAL OF MATERIALS SCIENCE 23 (1988) 4487–4491

Properties of $SbCl_5$-doped PPP/PPS composites

Part 2 *Surface mechanical behaviour*

D. R. RUEDA, F. J. BALTÁ CALLEJA, J. M. AYRES DE CAMPOS*, M. E. CAGIAO
Instituto de Estructura de la Materia, CSIC, Serrano 119, 28006 Madrid, Spain

Microindentation hardness is used to characterize the surface mechanical behaviour of two series of sintered PPP/PPS composites in a wide range of compositions. This work complements a previous electrical conductivity study carried out to determine the insulator–conductor transition within these materials. The influence of annealing the PPP-phase at 400° C before sintering the composites is discussed with reference to the additivity of hardness values of the single components PPP and PPS. The hardening of these composites upon doping with $SbCl_5$ is investigated in the light of the morphology of sintered materials. The elastic release of the material and the creep behaviour under the indenter are examined in terms of the porosity of the samples and of the dopant penetration within the material. In the case of compact materials, the hardness is found to increase due to a doping-induced surface-hardening effect. The hardness increase in porous materials responds to an inclusion of the dopant species within the material volume.

1. Introduction

In a preceding paper [1] (Part I) the investigation of the conductivity behaviour of $SbCl_5$-doped Polyparaphenylene/polyparaphenylene sulphide (PPP/PPS) sintered materials, was reported. This study was envisaged as an attempt to develop a route for obtaining conductive composite organic materials with improved mechanical properties. Previous attempts to obtain composites from other conducting polymers blended with insulating matrices have been reported elsewhere [2–7]. In Part I [1] attention was focused on the role played by the surface morphology of the composites, the relative weight variation upon doping and the stability of electrical conductivity, σ, during storage time. It was, further, shown that these sintered materials exhibit a discontinuous transition from non-conductor to conductor at about 20% wt of PPP. The influence of annealing of the PPP component at 400° C, prior to sintering, on the σ level was also examined.

In the present paper (Part II) the surface mechanical properties of these composite materials, before and after doping, have been investigated as revealed by microindentation hardness. A knowledge of the microhardness is critical if improvements in the surface mechanical and conducting properties, depending on materials processing and doping procedures, is to be made. It is known that microhardness (MH) is directly correlated to bulk properties [8] and that it can also provide useful information about a variety of microstructural changes in polymers produced by mechanical processing [9] and by chemical treatments [10–12].

The aim of the present work is to report: firstly on the MH variation of the sintered composites as a function of composition range, secondly, on the influence of annealing PPP at 400° C, before sintering, on the MH value, and thirdly on the change of MH after doping with $SbCl_5$ vapour. The elastic release and creep behaviour of the material surface under the indenter are also discussed in connection with the doping process of the composites.

2. Experimental part

2.1. Materials

The synthesis of PPP, the preparation of sintered composites using PPS as a matrix and the doping procedure were described in detail in Part I [1]. Two types of PPP were used as a conducting component: (a) PPP as synthesized (to be called PPP), and (b) PPP annealed at 400° C, (PPPa). Since PPP cannot be processed from the melt, for the hardness investigation $\approx 600\,\mu m$ thick platelets obtained by sintering the mixtures of the components in powder form, were prepared by compression at 0.75 GPa. Sintering involves material transfer through the interparticle regions leading to shrinkage of the sample and smoothing of particles which initially may have had uneven shapes. In Part I [1] we showed that original sintered PPP is a compact homogeneous material consisting of a compressed assembly of flat globular particles of 1–2 μm diameter (Fig. 1a). Sintered PPPa (Fig. 1b) exhibits, on the contrary, a rather rough surface composed of looser particles showing sharp edges separated by many microvoids of up to 1 μm in

* *Permanent address*: Physics Department, Universidade do Minho, Braga, Portugal.

0022–2461/88 $03.00 + .12

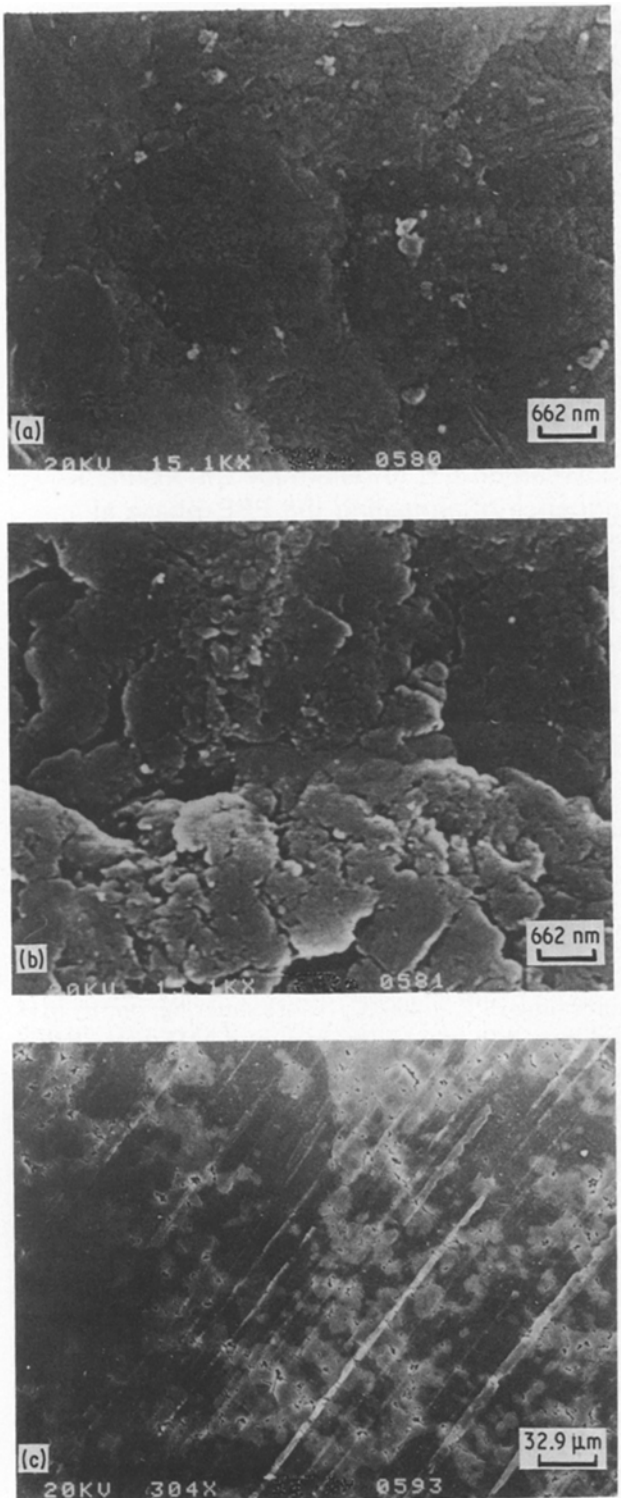

Figure 1 Scanning electron micrograph of (a) sintered PPP, (b) sintered annealed PPP, (c) sintered PPP/PPS composite (50 : 50). The lighter areas correspond to the PPS component showing the presence of micropores.

size. The annealing treatment modifies the surface of the particles lowering, as a result, the capacity of material transfer upon sintering through the inter-particles' surface. In other words, the PPP sintered samples are compact materials and the PPPa ones are more porous. Sintering of PPP with PPS particles gives rise to a dispersion of the PPP particles within the PPS matrix (Fig. 1c). The PPS particles (light areas) in Fig. 1c also exhibit the presence of great many micropores. After sintering both PPP and PPPa components with PPS in the whole range of compositions, simultaneous doping of both PPP/PPS (A) and PPPa/PPS (B) series was carried out by exposing the composites to vapour pressure of $SbCl_5$ for 21 h. Table I summarizes the materials investigated.

TABLE I Materials investigated

Sintered composites	PPP/PPS	PPPa/PPS
Before doping	A	B
After $SbCl_5$ doping	A′	B′

2.2. Techniques

The surface hardness was measured at room temperature using a Leitz microhardness tester with a Vickers square pyramidal diamond. The hardness of doped samples was measured after one month storage of the materials in air. These data correspond to levelling off values of the relative weight and conductivity data [1]. The hardness value was calculated according to

$$\mathrm{MH} = KP/d^2 \quad (\mathrm{MN\,m^{-2}}) \qquad (1)$$

where d is the length of impression diagonal, P is the contact load and K a geometrical factor equal to 1.854. Owing to the heterogeneity of the samples the accuracy of a MH determination from a series of 15–20 indentations lies, within 5–10%. In order to average adequately the experimental hardness data of the sintered composites a load of 1 N was mainly used. This load gives indentation diagonals in the range of 85–145 μm, thus, covering surface areas containing both PPP and PPS regions. To test the elastic release of the materials loads of 0.25, 0.5, 1 and 2 N were also applied. The loading time was 0.25 min. However, the time dependence of MH on the loading time was also investigated in selected cases in order to examine the creep behaviour of the material [13].

3. Results and discussion

3.1. Microhardness of sintered materials

The obtained MH value (using a load of 1 N) for the starting sintered PPP compact material is about 122 $\mathrm{MN\,m^{-2}}$ (Fig. 2). PPP samples supplied by Dr Froyer were also sintered in our laboratory and yield hardness values in the vicinity of our measured data ($\approx 110\,\mathrm{MN\,m^{-2}}$). When using annealed PPPa particles the porous morphology of the sintered material, gives rise to a MH value near 72 $\mathrm{MN\,m^{-2}}$. Finally, the microhardness of the PPS sintered matrix

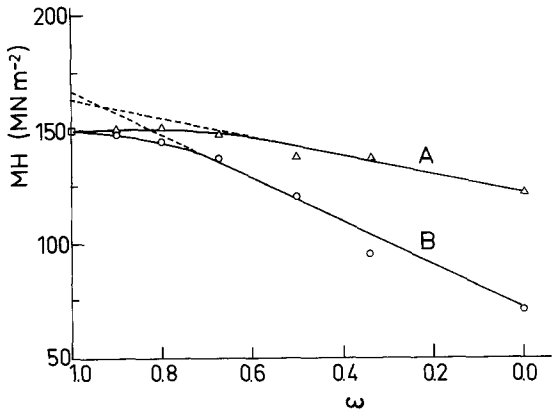

Figure 2 Microhardness of sintered PPP/PPS (A) and PPPa/PPS (B) composites as a function of weight compositions w. Load applied 1 N.

shows a value of 150 MN m^{-2}. Since MH is directly correlated to the density of a material [14], the above results are consistent with the fact that the crystal density of PPS (1.43 g cm^{-3}) [15] is higher than that of PPP (1.34 g cm^{-3}) [16]. The MH for the three sintered components was found to follow Equation 1 for $P \leqslant 3$ N (see below Fig. 4). Fig. 2 illustrates the gradual increase of MH as a function of PPS weight per cent concentration for both A and B series. The MH of polymer blends has been previously described in terms of a simple additive model system [17]

$$\mathrm{MH} = H_1 w + H_2(1 - w) \qquad (2)$$

where H_1 and H_2 and w and $(1 - w)$ are respectively the hardness values and weight fractions of the single components. For both series a deviation from the additivity law (Equation 2) is obtained. Extrapolation of the straight sections of the plot of Fig. 2 for 100% PPS ($w = 1$) yields a hardness value H_1 near ~ 167 MN m^{-2}. From here one may imply a material deficiency, MH/H_1, for the sintered PPS component of about $\sim 10\%$. This deficiency is due to the presence of a great many microvoids of 1–5 μm in diameter which makes the material weaker. Hence, the deviation of MH from the additivity law (Equation 2) for $w > 0.7$ can be interpreted in terms of a fraction of microvoids which is depressing the H_1 value. The fact that for $w < 0.7$ the MH data accommodate to the additivity behaviour of Equation 2 could be attributed to the filling of PPS micropores by PPP (or PPPa) material during the sintering process. Energy dispersive X-ray analysis for antimony across the platelet thickness for A series confirms, indeed, that for $w \leqslant 0.5$ the dopant does not penetrate into the material, remaining preferentially localized at the surface. The linear portion of the MH against w plot for series B in Fig. 2 similarly suggests a filling of PPS microvoids by the PPPa material.

3.2. Microhardness of doped materials

The influence of $SbCl_5$-doping upon the hardness of the composites is shown in Fig. 3. Perhaps, the most striking feature here is that the MH value for the PPP, PPPa and PPS single sintered components substantially increases after doping. The MH variation of PPP/PPS (A′) and PPPa/PPS (B′) composites after doping is markedly different. Thus, the B′ series now shows a linear increase of MH with w which is nearly parallel to the linear rise obtained for undoped B samples (Fig. 2). On the other hand MH for the A′ series remains nearly constant up to $w = 0.8$ and then suddenly increases up to ~ 225 MN m^{-2} for $w = 1$. The linear increase for the PPPa/PPS porous composites in the whole range of w can be explained in terms of a hardening of intergrain microvoids due to dopant penetration through micropores within the material volume [1]. Micropores appear specifically within the PPPa and PPS components throughout the composition range. A similar hardening has been obtained after etching polyethylene with chlorosulphonic, sulphuric and nitric acids [10–12].

Since in the compact PPP/PPS series the doping reaction for $w < 0.8$ is preferentially localized at a 5 μm surface (1) the hardening of the material is nearly

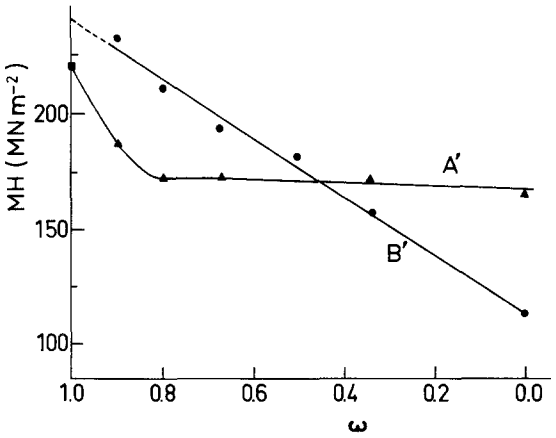

Figure 3 Microhardness of $SbCl_5$ doped sintered composites A′ and B′ after storage at ambient atmosphere for more than one month, as a function of weight composition. Load applied 1 N.

constant within this composition range. For $w > 0.8$, however, the influence of microvoids within the PPS volume partially filled with the dopant can explain the final hardness increase up to a value of ~ 225 MN m^{-2}.

3.3. Elastic release and creep behaviour

In order to further clarify the different behaviour between compact (A) and porous (B) samples we illustrate the variation of applied load P against the squared identation diagonal d^2 according to Equation 1 for the two composites with $w = 0.33$, before (open symbols) and after (filled symbols) doping (Fig. 4). Similar results were obtained for materials with other compositions. The material with a porous microstructure (B series) shows an intercept at the origin which is related to the instant elastic recovery of the composite after load removal [13]. The same intercept value is obtained for the material after doping. However, we have observed that the elastic release increases with the content of PPPa (i.e. with the density of micropores) up to a value of 0.07 N. Such an increase seems to support the concept that micropores induce the material to be compressed elastically under the indenter, releasing subsequently upon load removal. The hardening of the material observed after doping is reflected by the distinct slope increase (solid data

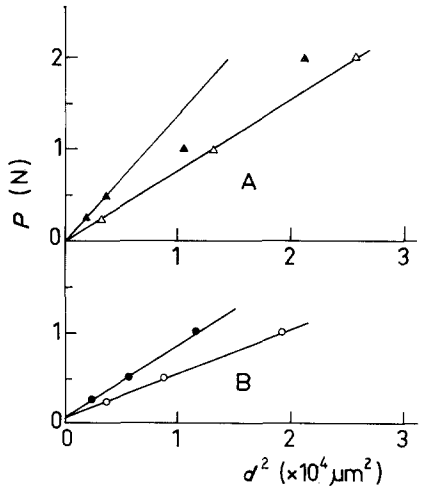

Figure 4 Load P plotted against square of indentation for the A and B composite samples with 33% wt of PPS, before (open symbols) and after (filled symbols) $SbCl_5$ doping.

in Fig. 4). The undoped compact composites of the PPP/PPS series (A samples) behave like ideal plastic materials, i.e. the plot of P against d^2 plot passes nearly through the origin. The thickness of the doped surface of the A′ composite series is about 5 μm. For the smallest load used, 0.25 N, the penetration depth of the indenter is, thus, similar to the thickness of the doped layer. However, for higher loads the penetration depth is clearly larger than the thickness of the $SbCl_5$-modified layer. Hence with increasing load one detects in Fig. 4, for A′ samples, a deviation from the expected linear behaviour of P against d^2, indicating that for higher P values one obtains apparently lower hardness values.

In case of the doped PPP/PPS (A′) samples, from the data derived using a load of $P = 0.25$ N, one may attempt to deduce an approximate microhardness value for the thin doped film surface, H_f. Smaller loads could not be used owing to the heterogeneity and uneven nature of the composites surface. The obtained value for H_f of 250 MN m^{-2} is, thus still affected by the MH of the substrate H_s [18]. The value of H_f also applies to doped PPP and is similar to the extrapolated value of the PPPa/PPS (B′) samples for $w = 1$. Therefore, the nearly constant result of ~ 170 MN m^{-2} for the A′ series in Fig. 3 represents nothing other than a depressed value because the load used was 1 N.

It is noteworthy, that from the geometry of the Vickers' indenter ($d = 7h$; h is the penetration depth), assuming for the hardness of the doped A materials, H_{doped}, an additive partitioning of the hardness values H_f and H_s

$$H_{doped} = 49KP/(h_f + h_s)^2 \quad (3)$$

one can derive the thickness of the hardened thin surface of these materials. For A′ composites with $w \leqslant 0.5$, by using loads of 1 and 2 N, a value of $h_f \sim 5\,\mu$m is obtained, in agreement with the thickness value previously reported [1].

The time dependent part of the plastic deformation of the material surface under the stress of the indenter, follows a law of the form [8]

$$MH = MH_0 t^{-k} \quad (4)$$

where, t is the loading-time, k a constant which measures the rate of creep of the material and MH_0 is a reference hardness value which depends on temperature and microstructure. Fig. 5 illustrates a plot of log MH against log t according to Equation 4 for the sintered PPP and PPPa components. Values of the creep constant, k, for some materials, before and after doping, are collected in Table II. These data show that: (1) porosity occurring within the PPS component

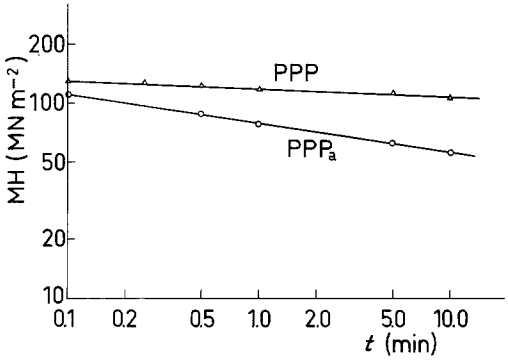

Figure 5 Log–log plot illustrating the loading time dependence of microhardness for the sintered PPP and PPPa components. Load applied 0.25 N.

and in the PPPa materials (B) induces an increase of k, (2) doping of both A and B series results in a similar increase of the k value. Creep is generally the result of stress induced internal transport by means of material diffusion [19]. On the other hand, creep in a sintered material can also respond to the phenomenon of grains sliding along each other. The above data suggest that sliding is activated by both the presence of micropores (series B) and by the inclusion of the dopant between the grains (series B′). This suggests that although the material becomes harder, after doping, the intercalated species might facilitate slippage rate between microparticles under the indenter. This result is in contrast with data obtained when doping polyethylene with chlorosulphonic acid [10] and nitric acid showing a decrease of k. The above increase of k in both series could be consistent with the fact that no chemical fixation of dopant molecules within PPP grain boundaries takes place during doping [1].

4. General conclusions

Composites of PPP with PPS have been attempted to improve the processability of conducting PPP. PPS is a versatile commercial material and its mechanical properties are partly retained when blended with PPP. The hardness of PPP/PPS sintered composites can be described in terms of an additive system of two independent components H_1 and H_2 for weight concentrations of PPS lower than 70%. For PPS weight concentrations larger than 70% the presence of micropores within the PPS component provokes deviations of the MH additive behaviour of the single components. Exposure of these composites to a $SbCl_5$ atmosphere for PPP compositions larger than 20%, improves both the electrical conductivity (as reported in Part I) in the range of 10° Ω^{-1} cm^{-1}, and the surface microhardness to values of ~ 175 MN m^{-2}, in the vicinity of those of some metals. The use of annealed PPP in the sintered composites gives rise to materials with a

TABLE II Creep constant, k (Equation 4) for the sintered composites investigated

Material	Weight composition	Before doping	After $SbCl_5$ doping
PPP/PPS	0:100	0.09	0.13
PPP/PPS	20:80	0.06	0.08
PPP/PPS	50:50	0.03	0.04
PPP/PPS	100:0	0.04	0.05
PPPa/PPS	33:67	0.03	0.06
PPPa/PPS	67:33	0.08	–
PPPa/PPS	100:0	0.15	–

large amount of micropores which after doping show similar conductivity levels and microhardness values. These values are not restricted to the material surface but are representative of the material volume. Exposure of the composites to ambient atmosphere after long storage times (several days) reduces the conductivity level by several orders of magnitude (Part I). The hardness values for the conducting composites quoted in this work were measured after one month storage and are much larger than the values for the undoped materials.

Acknowledgements

We would like to thank Dr Froyer (CNET, Lannion, France) for kindly giving us PPP specimens to compare with our own hardness data. Grateful acknowledgment is due to CAICYT, Spain, for the generous support of this work.

References

1. D. R. RUEDA, M. E. CAGIAO, F. J. BALTÁ CALLEJA and J. M. PALACIOS, *Synt. Met.* **22** (1987) 53.
2. M. E. GALVIN and G. E. WNEK, *Polymer* **23** (1982) 795.
3. G. L. BAKER and F. S. BATES, *Macromolecules* **17** (1984) 2619.
4. A. NAZZAL and G. B. STREET, *J. Chem. Soc. Chem. Commun.* (1984) 83.
5. M. A. de PAOLI, R. J. WALTMAN, A. F. DIAZ and J. BARGON, *J. Polym. Sci. Polym. Chem. Ed.* **23** (1985) 1687.
6. B. WESSLING, *Kunststoffe* **6** (1985) 375.
7. M. ALDISSI and A. R. BISHOP, *Polymer* **26** (1985) 622.
8. F. J. BALTÁ CALLEJA, *Adv. Polym. Sci.* **66** (1985) 117.
9. D. R. RUEDA, F. J. BALTÁ CALLEJA and R. K. BAYER, *J. Mater. Sci.* **16** (1981) 3371.
10. J. MARTINEZ SALAZAR, D. R. RUEDA, M. E. CAGIAO, E. LÓPEZ CABARCOS and F. J. BALTÁ CALLEJA, *Polym. Bull.* **10** (1983) 553.
11. F. J. BALTÁ CALLEJA, C. FONSECA, J. M. PEREÑA and J. G. FATOU, *J. Mater. Sci. Lett.* **3** (1984) 509.
12. M. E. CAGIAO, D. R. RUEDA and F. J. BALTÁ CALLEJA, *Coll. Polym. Sci.* **265** (1987) 37.
13. F. J. BALTÁ CALLEJA, D. R. RUEDA, R. S. PORTER and W. I. MEAD, *J. Mater. Sci.* **15** (1980) 765.
14. F. J. BALTÁ-CALLEJA, D. R. RUEDA, J. GARCIA, F. P. WOLF and W. H. KARL *ibid.* **21** (1986) 1139.
15. P. PRADERE, A. BOUDET, J. Y. GOBLOT, G. FROYER and F. MAURICE, *Mol. Cryst. Liq. Cryst.* **118** (1985) 277.
16. B. J. TABOR, E. P. MAGRE and J. BOON, *Eur. Polym. J.* **7** (1971) 1127.
17. J. MARTINEZ SALAZAR and F. J. BALTÁ CALLEJA, *J. Mater. Sci. Lett.* **4** (1985) 324.
18. P. J. BURNETT and D. S. RICKERBY, *Thin Solid Films* **148** (1987) 41.
19. H. G. van BUEREN, "Imperfections in Crystals", 2nd Edn, (North Holland, Amsterdam, 1961) p. 236.

Received 20 November 1987
and accepted 3 March 1988